CSIRO PUBLISHING www.publish.csiro.au/journals/eg Copublished paper, please cite all three:
Exploration Geophysics, 2009, **40**, 121–131; *Butsuri-Tansa*, 2009, **62**, 121–131; *Mulli-Tamsa*, 2009, **12**, 121–131

Experiments on the stability of the spatial autocorrelation method (SPAC) and linear array methods and on the imaginary part of the SPAC coefficients as an indicator of data quality

Sos Margaryan[1,3] Toshiaki Yokoi[1] Koichi Hayashi[2]

[1]International Institute of Seismology and Earthquake Engineering, Building Research Institute, 1 Tachihara, Tsukuba, Ibaraki 305-0802, Japan.
[2]OYO Corporation, 43 Miyukigaoka, Tsukuba, Ibaraki 305-0802, Japan.
[3]Corresponding author. Email: msos78@hotmail.com

Abstract. In recent years, microtremor array observations have been used for estimation of shear-wave velocity structures. One of the methods is the conventional spatial autocorrelation (SPAC) method, which requires simultaneous recording at least with three or four sensors. Modified SPAC methods such as 2sSPAC, and linear array methods, allow estimating shear-wave structures by using only two sensors, but suffer from instability of the spatial autocorrelation coefficient for frequency ranges higher than 1.0 Hz.

Based on microtremor measurements from four different size triangular arrays and four same-size triangular and linear arrays, we have demonstrated the stability of SPAC coefficient for the frequency range from 2 to 4 or 5 Hz. The phase velocities, obtained by fitting the SPAC coefficients to the Bessel function, are also consistent up to the frequency 5 Hz. All data were processed by the SPAC method, with the exception of the spatial averaging for the linear array cases. The arrays were deployed sequentially at different times, near a site having existing Parallel Seismic (PS) borehole logging data.

We also used the imaginary part of the SPAC coefficients as a data-quality indicator. Based on perturbations of the autocorrelation spectrum (and in some cases on visual examination of the record waveforms) we divided data into so-called 'reliable' and 'unreliable' categories. We then calculated the imaginary part of the SPAC spectrum for 'reliable', 'unreliable', and complete (i.e. 'reliable' and 'unreliable' datasets combined) datasets for each array, and compared the results. In the case of insufficient azimuthal distribution of the stations (the linear array) the imaginary curve shows some instability and can therefore be regarded as an indicator of insufficient spatial averaging. However, in the case of low coherency of the wavefield the imaginary curve does not show any significant instability.

Key words: imaginary spatial autocorrelation coefficient, linear array, microtremor, spatial autocorrelation, stability.

Introduction

The frequency-wavenumber (*f-k*) and spatial autocorrelation (SPAC) methods are data processing techniques for processing microtremor array measurements to obtain phase velocities. The basic theory of the SPAC method was proposed by Aki (1957). Okada (1998, 2003), and Okada et al. (1990) developed the theory to determine phase velocities of Rayleigh and Love waves in a conventional way as an exploration method, by using horizontal and vertical components of microtremor array observations. To extract the Rayleigh wave, both methods require simultaneous recording of the vertical component of microtremors, with at least three or four sensors for the SPAC method and six or seven sensors for the *f-k* method (Capon, 1969; Asten and Henstridge, 1984; Horike, 1985).

In comparison with the SPAC method, the *f-k* method allows irregular array geometry, which makes it attractive. However, although the SPAC method requires circular or triangular arrays, it requires fewer sensors and data analysis is simpler. Ling and Okada (1993) proposed the extended spatial autocorrelation (E-SPAC) method, which allows obtaining the phase velocity by fitting the SPAC coefficients to a Bessel function versus distance, from several different shaped arrays deployed not simultaneously, but at different times. Moreover, according to Ohori et al. (2002), the E-SPAC method seems to have potential to provide more accurate results than the *f-k* method. In addition, Tsuno and Kudo (2004) showed the efficiency and precision of the SPAC method in practical engineering use, especially for shallow depths of investigation.

Morikawa et al. (2004) proposed an alternative SPAC method, called the 'two-site SPAC (2sSPAC) method', which requires only two sets of seismographs, one at a fixed and the other pivoting over the vertexes of the triangular array, under the assumption that the wave fields are spatially and temporally stationary. They concluded that the 2sSPAC method provides reasonable values for phase velocities in the frequency range lower than ~1.0 Hz, and noted that the spatial autocorrelation coefficients were not stable in the frequency range higher than 1.0 Hz.

Margaryan (2006) verified the accuracy and applicability of the 2sSPAC method for 50 m and 100 m equilateral triangular arrays, using seven sensors. The dispersion curves obtained by the SPAC and 2sSPAC methods were compared and showed good agreement up to 2.3 Hz.

Chavez-Garcia et al. (2006) proposed another modification to the SPAC method, in which they deployed seismometers at different inter-station spacing (5 m, 10 m, 20 m, and 40 m) along a line. They concluded that use of the SPAC method is not restricted to a particular geometry of the array, provided that the basic requirement of stationarity is fulfilled.

 10.1071/EG08101 0812-3985/09/010121

The results obtained by the SPAC method depend on the quality of the recorded data. The data can be qualified as good, if two main conditions are met, these being the quality of signal coherency between stations, and azimuthal coverage (or spatial averaging) of the array used.

According to Asten (2006) the imaginary part of the SPAC spectrum may provide quality control where single pairs of sensors are used over extended recording times. Asten (2006) has shown that for typical triangular array the azimuthal distributions of wave energy should be on the order of 60° or greater to have a high probability of being free of perturbations of the SPAC spectrum. As a solution, in case of insufficient azimuthal distribution of energy for a wide range of frequencies, he suggested using a six-station semicircular array.

However, Okada (2006) theoretically proved that three-station circle array, when compared with four-, five-, or nine-station arrays, is the most efficient and favourable for observation of microtremors, if the SPAC coefficients are used up to a frequency at which the coefficient takes the first minimum value.

The practical aim of this study is to show the stability of conventional SPAC and linear array methods, for a frequency range higher than 1.0 Hz, and to verify that the imaginary part of SPAC coefficients is useful as an indicator of data quality. For these purposes we carried out array observations of microtremors with four different-sized triangular arrays, and four same-size triangular and linear arrays, which were deployed sequentially at different times, but located close to each other and near a site having existing Parallel Seismic (PS) logging data.

Field configurations of microtremor arrays

Our experiments on array observations of microtremors, using different sized arrays, were carried out in Tsukuba city, located in the Kanto Basin, Japan, where Parallel Seismic (PS) logging data up to depths of 1300 m is also available (Suzuki and Takahashi, 1999). For simplicity we term 200 m, 150 m, 100 m, and 50 m arrays 'middle' arrays, and the four 25 m arrays, 'small' arrays. In both cases measurements were conducted using circular (or triangular) arrays consisting of three stations on the circumference and one central station. For further analysis we used two distances, which are the distance between the central station and the stations located on the circumference, and the inter-station distance between the stations located on the circumference. For all arrays vertical-component velocity-type geophones, and MxSEIS-SXW OYO data acquisition recorders, were used, and data were synchronised by Global Positioning System (GPS) clocks. The geometry of the arrays is shown in Figure 1.

The 'middle' arrays

The geometry of the middle arrays is shown in Figure 1*a*. For these arrays L4C sensors with a natural frequency 1.0 Hz were used. Observation was done simultaneously first for the 50 m and 100 m arrays, then for the 150 m and 200 m arrays. The duration of the records for each array was ~32 min, divided into 60 datasets. The sampling interval was 0.002 s; each dataset includes 16 384 data points.

The 'small' arrays

For the small arrays L22D sensors with a natural frequency 2.0 Hz were used. The small arrays were deployed sequentially, with simultaneous observation by four stations in a triangular array as described above. The first array (Figure 1*b*, s1-s2-s4 triangle), was located a distance of ~25 m from a road. The duration of the microtremor records for each array was 11 min, obtained as

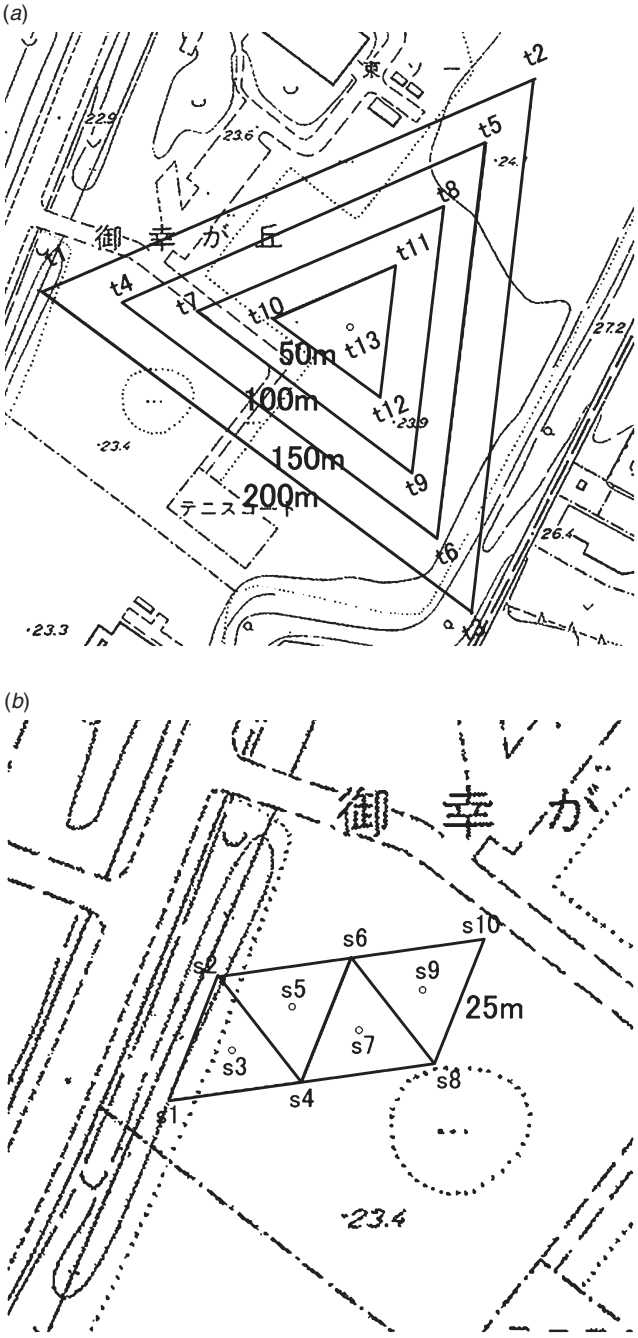

Fig. 1. Geometry of the arrays deployed. (*a*) Four triangle 200 m, 150 m, 100, 50 m arrays, (*b*) four triangular and linear 25 m arrays.

22 successive datasets each with a sampling interval of 0.002 s and length 16 384 points. We also used triangle sides labelled s1-s4, s4-s8, s2-s6, s6-s10 as linear arrays (Figure 1*b*).

Data analysis methods

SPAC and linear array methods

The SPAC coefficients, $\rho(\omega;r)$ can be directly calculated from the microtremor observed data using equation (1)

$$\rho(\omega;r)=\frac{1}{2\pi}\int_0^{2\pi}\frac{\mathrm{Re}\{[S_{CX}(\omega;r,\theta)]\}}{\sqrt{[S_C(\omega;0,0)]\cdot[S_X(\omega;r,\theta)]}}d\theta, \qquad (1)$$

where $\mathrm{Re}\{\cdot\}$ stands for the real part of a complex value, $S_C(\omega;0,0)$ and $S_X(\omega;\ r,\theta)$ are the power spectra of microtremor at

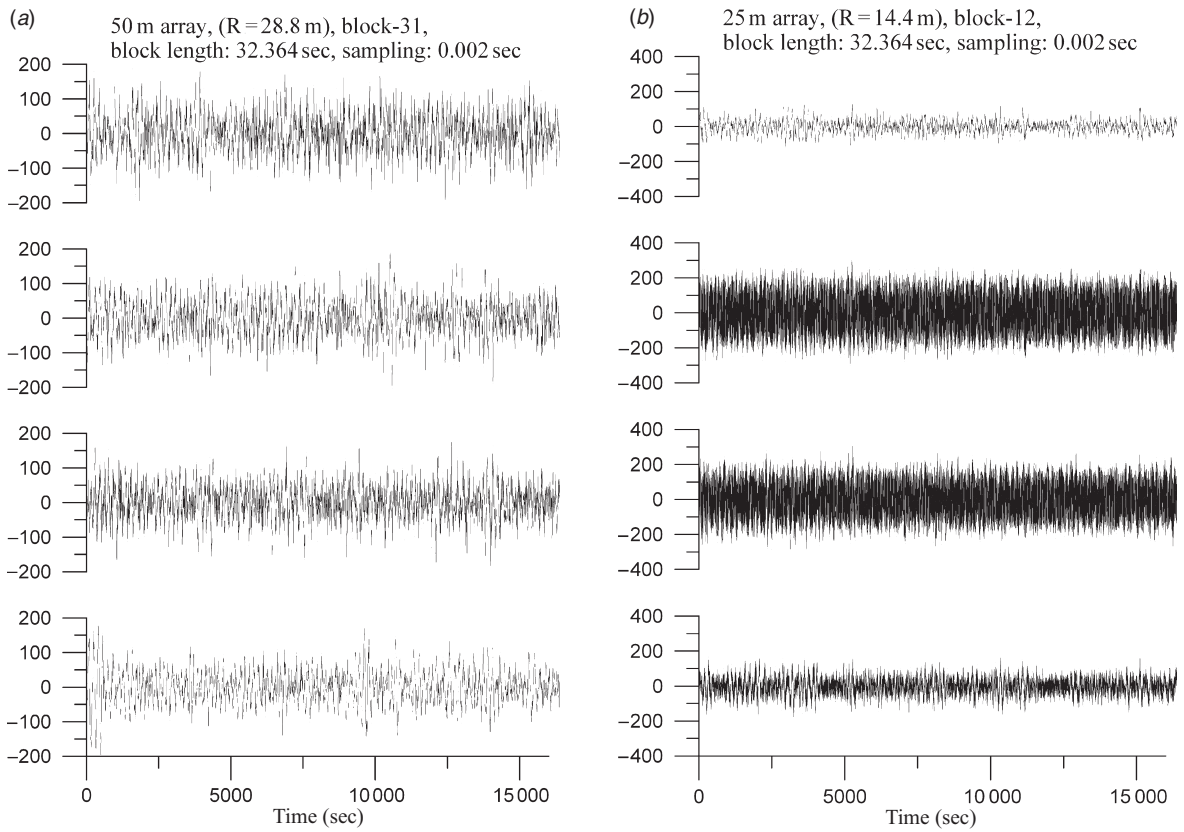

Fig. 2. Examples of microtremor velocity waveforms. (*a*) Record obtained from 50 m array. (*b*) Record obtained from the first 25 m array.

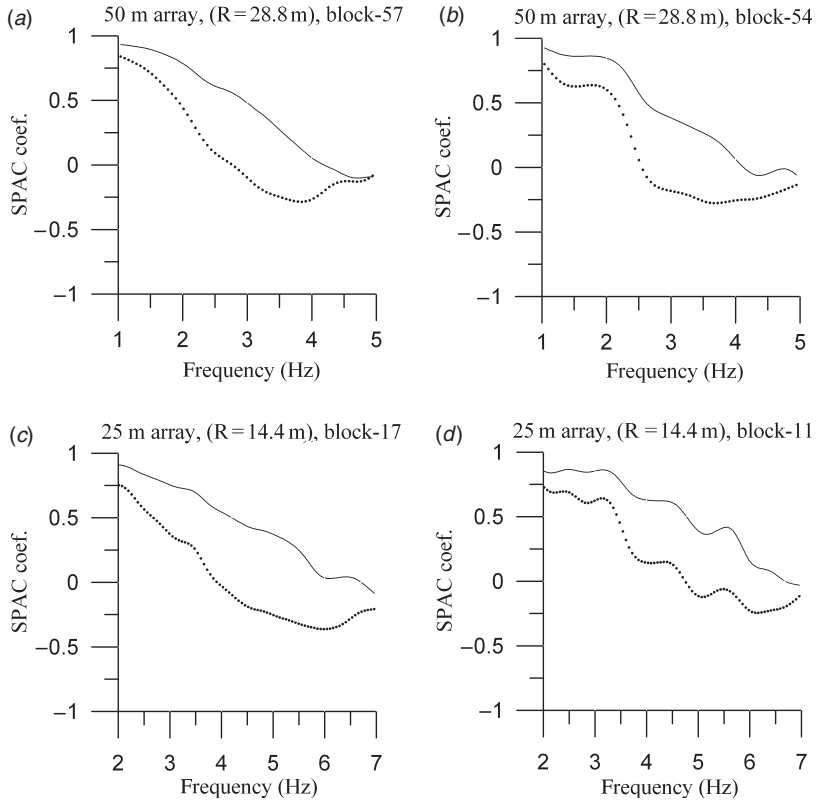

Fig. 3. Spatial autocorrelation (SPAC) coefficients for different datasets of the 50 m and the first 25 m arrays. (*a*) and (*b*) Dotted and thin lines are the SPAC coefficients obtained for 50 m and 28.8 m distances, respectively; (*c*) and (*d*) dotted and thin lines are the SPAC coefficients obtained for 25 m and 14.4 m distances, respectively. (*a*) and (*c*) are examples of data classified as 'reliable'. (*b*) and (*d*) have perturbations in the spectra and are examples classified as 'unreliable'.

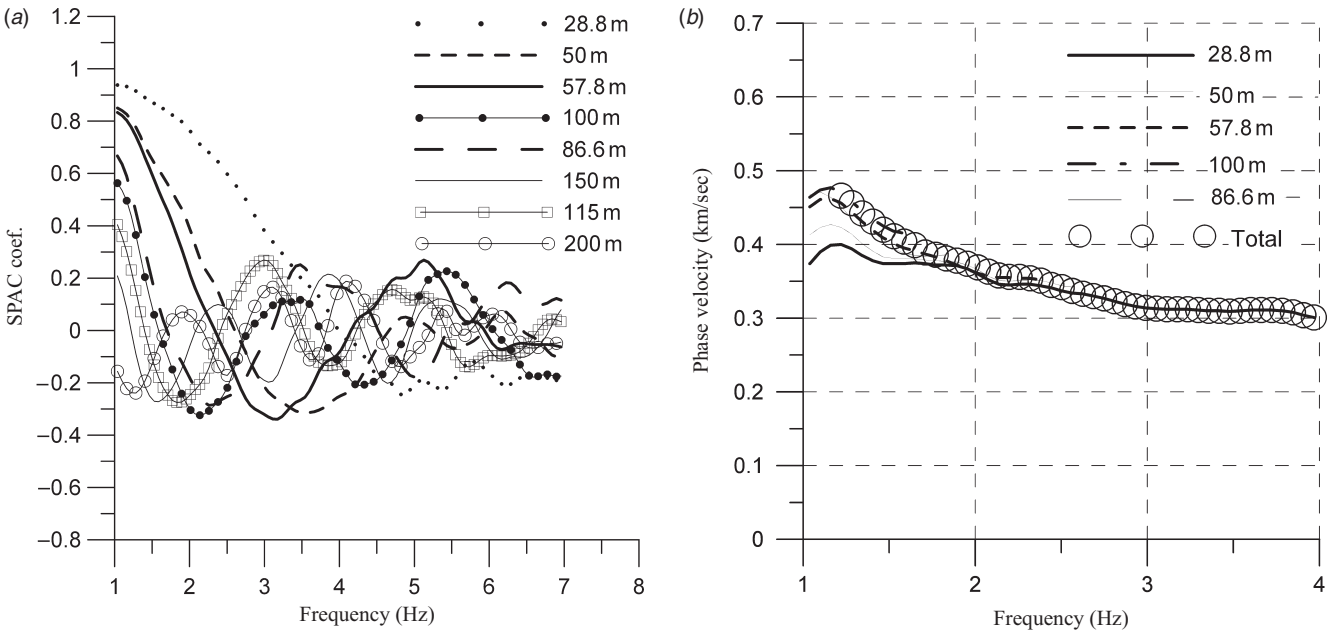

Fig. 4. Spatial autocorrelation (SPAC) coefficients and phase velocities obtained from the middle arrays. (*a*) Average autocorrelation coefficients obtained from all inter-station distances including in the middle arrays, (*b*) Solid lines show the observed phase velocities determined from inter-station distances including the middle arrays; the total observed phase velocity obtained by the extended spatial autocorrelation (E-SPAC) method shown by circles.

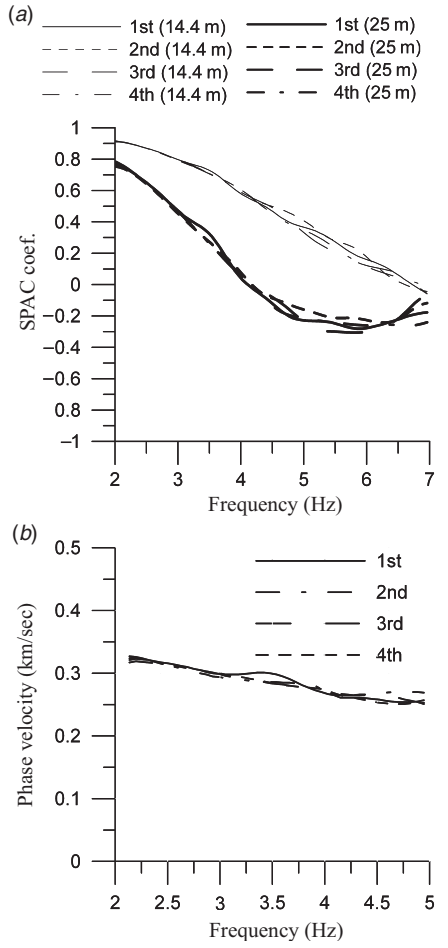

Fig. 5. Spatial autocorrelation (SPAC) coefficients and phase velocities obtained from four small arrays. (*a*) Thin and solid lines show average autocorrelation coefficients obtained from the 14.4 m and 25 m distances, respectively. (*b*) Phase velocities determined by the four small arrays.

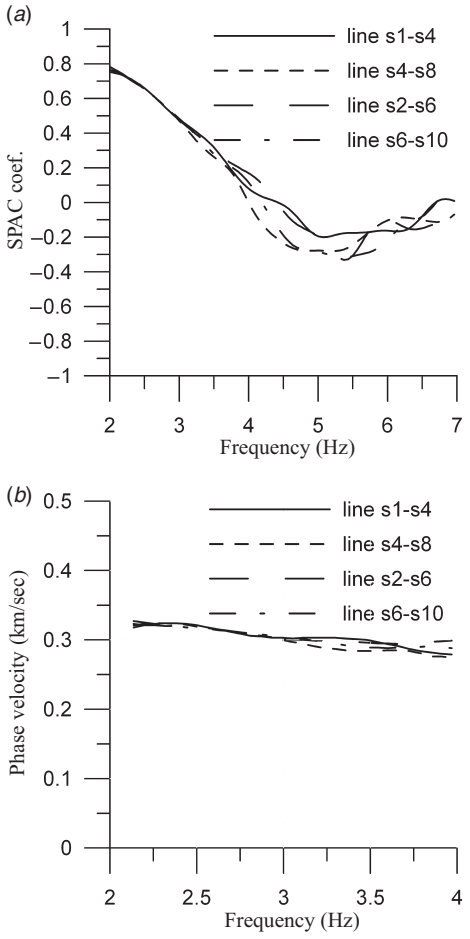

Fig. 6. Spatial autocorrelation (SPAC) coefficients and phase velocities obtained from four linear arrays. (*a*) Autocorrelation coefficients obtained from the pairs s1-s4, s4-s8, s2-s6, s6-s10 with distance of 25 m. (*b*) Phase velocities determined by the four linear arrays.

two sites C and X, respectively, and $S_{CX}(\omega; r,\theta)$ is the cross spectrum between the two sites, and [ ] denotes the block average over time.

For the linear arrays, based on the assumption that microtremors are travelling in multiple directions, the SPAC coefficients were calculated by using equation (1), but without averaging the cross-correlation coefficients azimuthally.

The imaginary part of the SPAC coefficient was calculated by modifying equation (1), replacing the real part of the cross spectrum with the imaginary part.

Phase velocity

Before making the phase-velocity calculation we visually examined the waveforms of the records and removed datasets

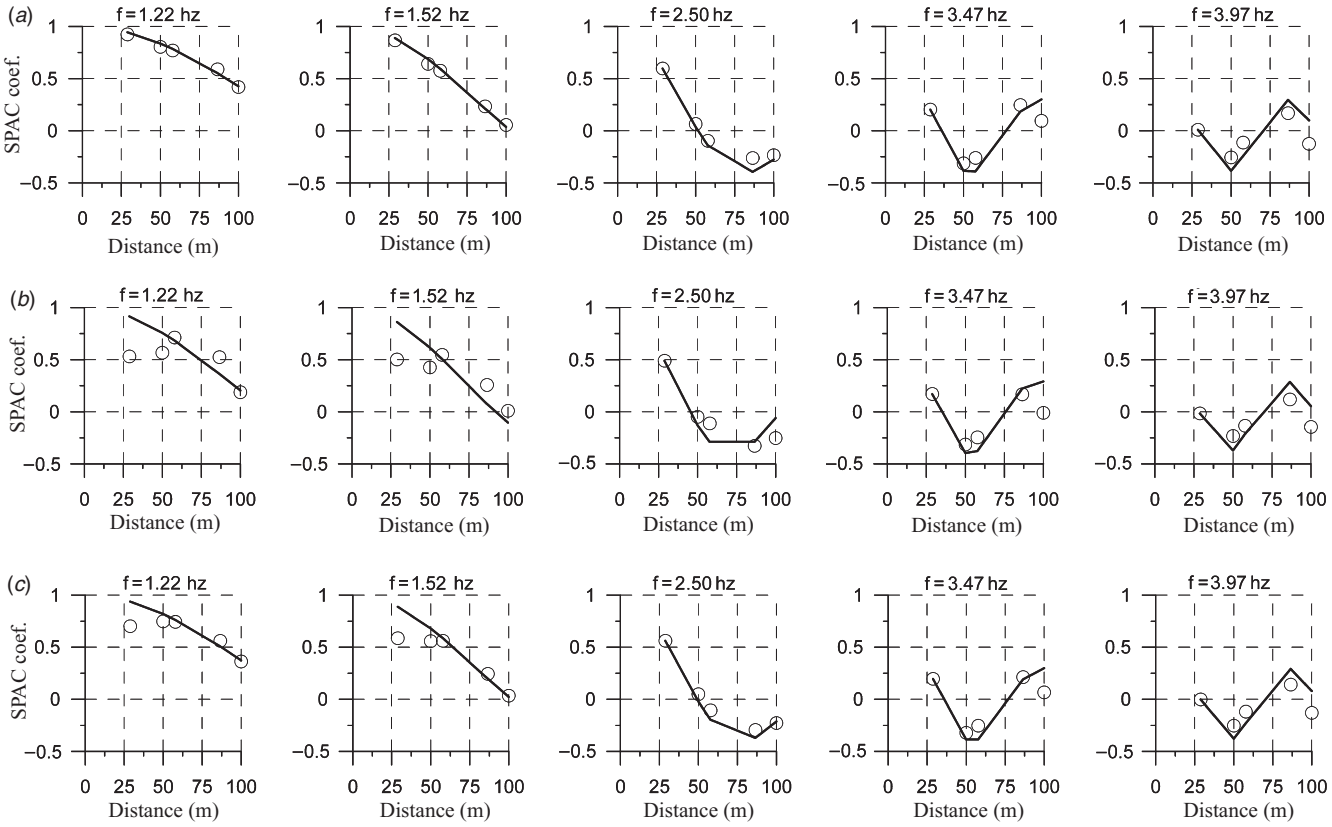

Fig. 7. An example of the SPAC coefficients fitted to the Bessel function for some frequencies (1.22 Hz, 1.52 Hz, 2.50 Hz, 3.47 Hz, and 3.97 Hz). The solid lines show the Bessel function and the circles indicate the SPAC coefficients: the examples shown in (*a*), (*b*), (*c*) are obtained by using 'reliable', 'unreliable' and complete datasets from the middle arrays, respectively.

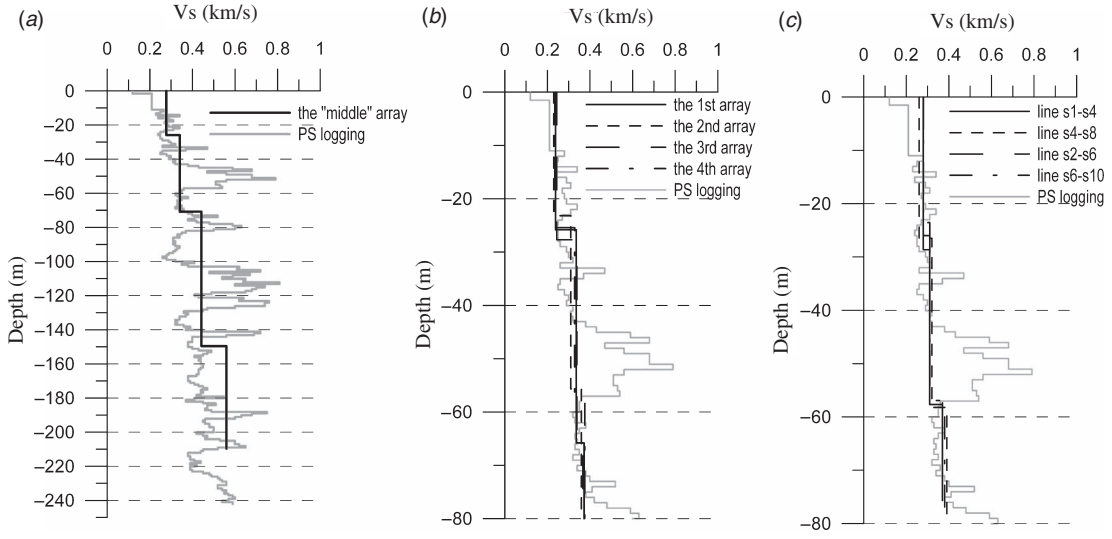

Fig. 8. Comparison of shear-wave velocity structures determined by array microtremors with the PS logging data (Suzuki and Takahashi, 1999) for (*a*) middle arrays, (*b*) small arrays and (*c*) linear arrays.

contaminated by noise such as traffic noise. This procedure was done only for the middle arrays, because the small-array records contained high-frequency interference noise generated from high-voltage lines passing above the investigation sites, and consequently it was difficult visually to distinguish which datasets were good or bad. Figure 2 shows examples of data blocks for ground-velocity recordings of microtremors, as obtained for the 50 m array, and for the first 25 m array.

Next, for the middle and small arrays we visually examined the SPAC spectra obtained from each dataset, and discarded datasets showing relatively significant perturbations. In Figure 3 examples of averaged autocorrelation functions obtained from a single dataset for the 50 m and the first 25 m arrays are shown. After examining the data quality in this way, the applicable datasets, so-called 'reliable' data (for example, Figures 3*a* and 3*c*), were used for further analysis and determination of shear-wave velocity structures, whereas the rest of the datasets having been classified as 'unreliable' (for example, Figures 3*b* and 3*d*) was used only for purposes of analysis of the imaginary part of the SPAC spectrum. In the discussion later, it is shown that 'reliable' datasets can give a stable estimate of phase velocity, whereas the 'unreliable' datasets do not, hence these terms indicate stable and unstable estimates of phase velocity, respectively.

The phase velocities were obtained by fitting the SPAC coefficients to the Bessel function of the first kind of zero order by using equation (2)

$$\rho(\omega; r) = J_0\left(\frac{\omega r}{c(\omega)}\right), \tag{2}$$

where $J_0(\cdot)$ is the Bessel function of the first kind with the zero order and $c(\omega)$ is the phase velocity at frequency ω for the fundamental mode of the Rayleigh waves. The phase velocity at frequency ω is obtained as the argument of the Bessel function.

Figures 4–6 show SPAC coefficients, calculated from 'reliable' datasets together with corresponding phase velocities of Rayleigh waves, as obtained from the middle, small, and linear arrays respectively.

Although the middle arrays include 200 m, 150 m, 100 m, and 50 m arrays, the final observed phase velocity obtained from the middle arrays (Figure 4*b*) was calculated by using only the 50 m and 100 m arrays, and the 86.6 m inter-station distance from the 150 m array. The remainder of the data from the middle arrays in

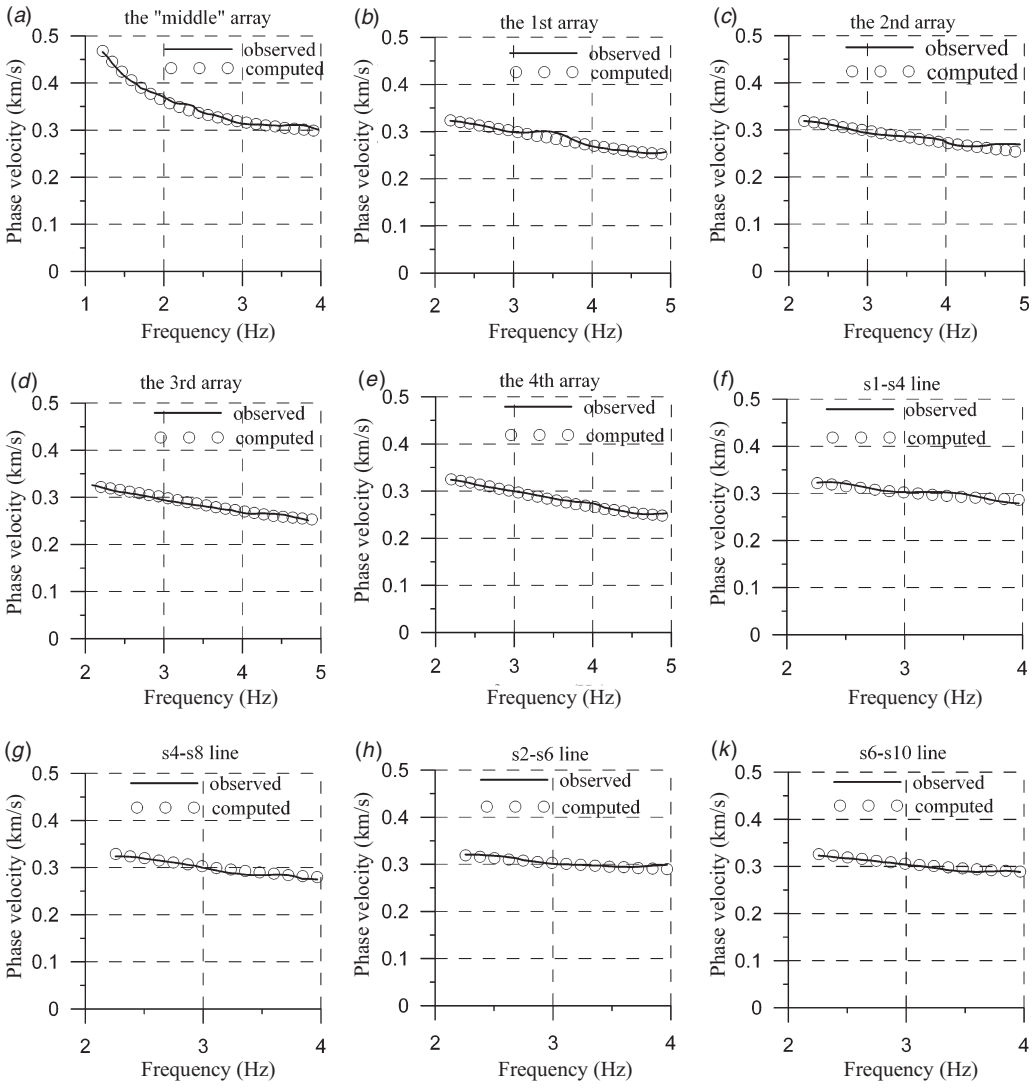

Fig. 9. Observed and computed phase velocities of Rayleigh waves; (*a*) for the middle arrays; (*b*), (*c*), (*d*), (*e*) for the small arrays; (*f*), (*g*), (*h*), (*k*) for linear arrays.

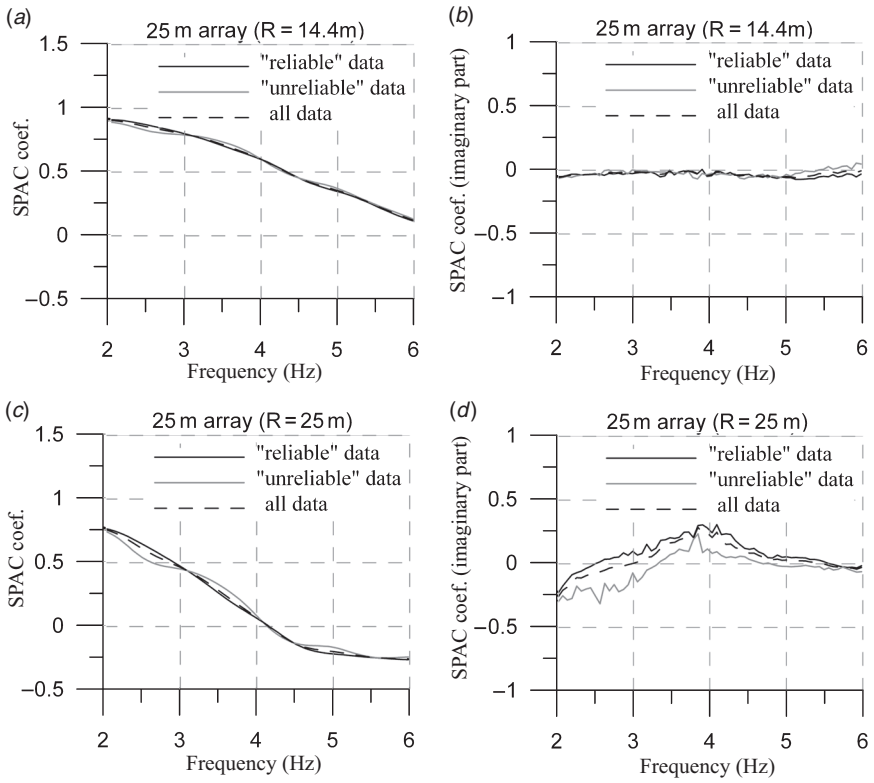

Fig. 10. The real and imaginary parts of the spatial autocorrelation (SPAC) coefficients for the fourth 25 m array obtained by all, 'reliable' and 'unreliable' datasets for two inter-station distances; (*a*) and (*c*) the real part of the SPAC coefficients for the 14.4 m and 25 m distances, respectively; (*b*) and (*d*) the imaginary part of the SPAC coefficients for the 14.4 m and 25 m distances, respectively.

the frequency range starting from 1.0 Hz showed lower coherency (Figure 4*a*) and was not used.

Fitting to the Bessel function

The quality of the calculated phase velocity is controlled by the degree of matching between the Bessel function of the first kind of zero order and the observed SPAC coefficients, plotted as a function of array spacing. This procedure allows verifying the values of the frequencies suitable for fitting. Figure 7 shows the examples of the SPAC coefficients fitted to the Bessel function for some representative frequencies for the 'reliable', 'unreliable' and complete datasets from the middle arrays.

Determination of shear-wave velocity structure

The inversion of the phase velocity to a shear-wave velocity structure is based on optimisation techniques such as the least-squares method or heuristic search algorithms. Known heuristic search algorithms which have been used for this type of inversion are the Genetic Algorithm (GA) method (Yamanaka and Ishida, 1996), and the Very Fast Simulated Annealing Method (VFSA) (Ingber, 1989). According to Yamanaka (2004), GA and VFSA show similar performance in convergence speed to find models near the optimal solutions; however, VFSA is good at finding models with smaller misfits than is the GA, because of the local search features of the VFSA.

The shear-wave velocity structures beneath the observation sites were inverted from the dispersion curves obtained by the middle, small, and linear arrays using a combination of the Down Hill Simplex method with VFSA (Yokoi, 2005), where layer thickness is changed independently of layer S-wave velocity in order to get the best fit.

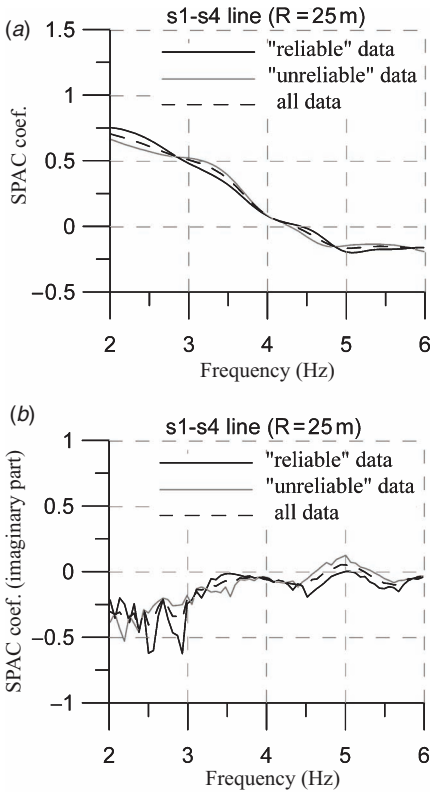

Fig. 11. The real and imaginary parts of the spatial autocorrelation (SPAC) coefficients for the s1–s4 linear array obtained by all, 'reliable' and 'unreliable' datasets for 25 m inter-station distance; (*a*) the real part of the SPAC coefficients for 25 m distance; (*b*) the imaginary part of the SPAC coefficients for 25 m distance.

The initial velocity-model parameters used in the inversions were the same for each array except for the middle array. The comparison of phase-velocity dispersions computed by VFSA with observed phase velocities obtained by SPAC and 2sSPAC methods is shown in Figures 9*b*–9*h*, and 9k, and shows good agreement in the observed frequency range.

Results

We conducted the microtremor measurements with 200 m, 150 m, 100 m, 50 m, and four 25 m triangular arrays. We use these measurements 1) to show the stability of the conventional SPAC and linear array methods for the frequency range higher than 1.0 Hz, and 2) to verify the imaginary part of the SPAC coefficients as a quality control indicator.

Assessment of the stability

The four sequentially deployed 25 m triangular arrays (small arrays), and four linear arrays made from the sides of triangles (which also can be regarded as a 2sSPAC method, because only two sensors have been used) have been used to verify the stability of the SPAC spectrum in the frequency range higher than 1.0 Hz. Results are presented in Figure 5*a*. This plot shows that the SPAC coefficients obtained from the four small arrays, for inter-tation distances 14.4 m and 25 m, are mutually consistent up to the frequencies of 4.3 and 6.75 Hz, respectively. The deviation at higher frequencies might be due to the dependence of sources on azimuth, but there is no data to verify this. The phase velocities, however, are mutually consistent up to the frequency of 5.0 Hz (Figure 5*b*). Although

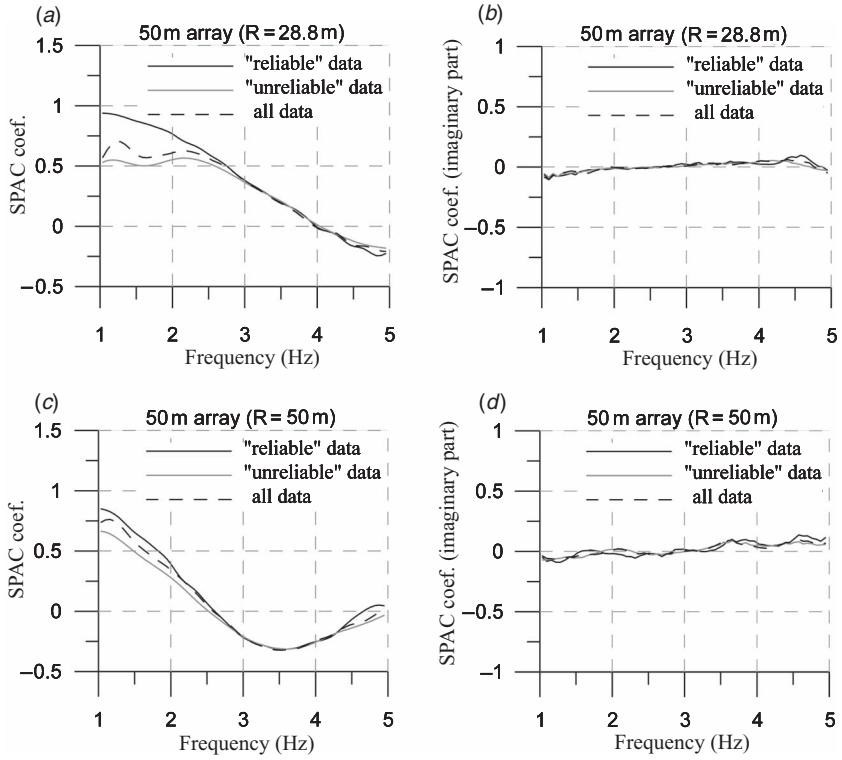

Fig. 12. The real and imaginary parts of the spatial autocorrelation (SPAC) coefficients for the 50 m of the middle arrays obtained by all, 'reliable' and 'unreliable' datasets; (*a*) and (*c*) the real part of the SPAC coefficients for the 28.8 m and 50 m distances, respectively; (*b*) and (*d*) the imaginary part of the SPAC coefficients for the 28.8 m and 50 m distances, respectively.

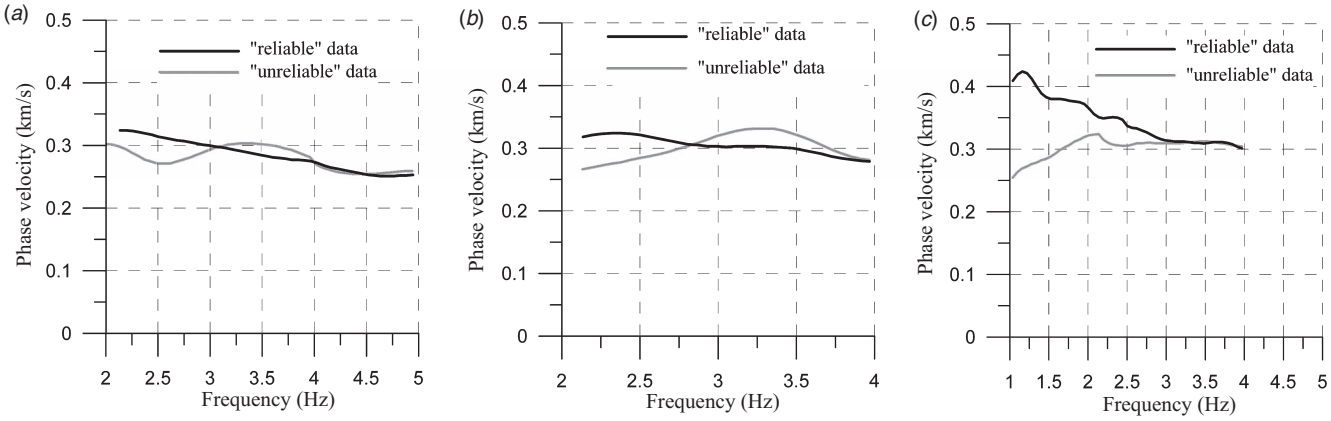

Fig. 13. Comparison of the phase velocities obtained from 'reliable' and 'unreliable' data: (*a*) for the fourth 25 m arrays; (*b*) for the s1-s4 linear array; (*c*) for the 50 m station separation of the middle arrays.

the SPAC coefficients obtained from the four linear arrays were not spatially averaged, they showed good stability up to ~3.9 Hz frequency, and it was possible to retrieve phase velocities up to the same frequency limit. Figures 6*a* and 6*b* show the consistency of the SPAC coefficients and phase velocities as obtained from the linear arrays for the 2.0 to 4.0 Hz frequency range.

Phase-velocity obtained from the inter-station distance 28.8 m of the middle arrays (Figure 4*b*), is also consistent with the phase velocities obtained by small and linear arrays in the frequency range from 2.0 to 4.0 Hz, which again confirms the stability of the SPAC coefficients obtained by two sensors only.

Assessment of estimated S-wave velocities

Figure 8 shows the shear-wave velocity structures obtained by the middle, small, and linear arrays together with existing PS logging data. The comparison of presented in Figures 8*a*–8*c* show the shear-wave velocity structures obtained from the middle, small, and linear arrays, respectively, together with the PS logging data. The agreement among all soil profiles obtained by the small and linear arrays is good. The information shows two sediment layers in the top 80 m. We can see that for depths ~23–27 m and 55–57 m the models are agree well with each other. Moreover, the shear-wave velocity model obtained by the middle arrays (Figure 8*a*) also agreed with models obtained by the small and linear arrays down to the 23–27 m depth boundary. Consistency between the shear-wave velocity profiles obtained and the PS logging data for the depths investigated is in general acceptable; however, there is some inconsistency at very shallow depths of ~10 m and less. The inconsistency is related to the array sizes and the frequency ranges of SPAC coefficients used; to obtain shear-wave velocity profiles at very shallow depths, we need additional short inter-station distances.

Assessment of data quality using the SPAC imaginary coefficients

In this section we assess the behaviour of the imaginary SPAC coefficients and compare differences between 'reliable' and 'unreliable' data when there are perturbations in the real parts of the SPAC coefficients. Using the hypothesis that perturbations on the SPAC coefficients can be generated by an insufficient azimuthal coverage of stations in an array we presented examples of the comparison for cases where the perturbations are relatively strong and obvious. Figures 10–12 show the real and imaginary parts for examples of 'reliable', 'unreliable', and complete datasets, for the fourth 25 m array, the s1-s4 linear array, and the 50 m middle array, respectively.

The comparison of the imaginary part of the SPAC coefficients calculated from the 'reliable', 'unreliable' and complete datasets does not show strong differences associated with the presence of strong perturbations on the real component of the SPAC spectrum, although Figure 11 for the linear array, where we expect perturbations associated with insufficient azimuthal averaging to be most evident, does show correlations in perturbations between real and imaginary parts of the SPAC spectrum in the frequency band 4 to 6 Hz. It seems that the differences between the real part of the SPAC coefficients obtained from the 'reliable' and 'unreliable' datasets are in general not large, but phase velocities obtained from the 'unreliable' datasets (Figure 13) show significant instability.

Figure 12 shows SPAC coefficients for the 50 m array (Figures 12*a*–12*d*) which show a different type of perturbation in the real SPAC coefficients, for frequencies below 2 Hz. There is a strong difference between the real part of the SPAC coefficients for 'reliable' and 'unreliable' data at frequencies less than 2 Hz. In this case the difference appears to be due to a loss of coherency rather than insufficient azimuthal averaging, and there is close to no difference in the corresponding imaginary parts of the SPAC coefficients.

Conclusions

We have analysed microtremor measurements from triangular and linear arrays by using SPAC and 2sSPAC methods respectively. The comparative analysis of the data showed good stability of the SPAC coefficients and phase velocities for frequency range from 2.0 to 4.0 Hz for linear arrays, and up to 5.0 Hz for triangular arrays. The results obtained from triangular arrays of different sizes are consistent with results obtained from the relatively small linear arrays for the same frequency ranges. Furthermore, the inverted shear-wave velocity profiles, obtained using the same initial model for all the arrays, are also in good agreement with each other, as well as with independent PS logging data.

We have considered use of two alternative criteria for determining data quality, first the presence of perturbations on the real part of the SPAC spectra, and second, non-zero behaviour of the imaginary part of the SPAC spectra. In this study the separation of datasets into 'reliable' and 'unreliable' was tentative based on observation of perturbations in the azimuthally-averaged autocorrelation spectrum, and in some cases on visual examination of the recorded waveforms. We also compared the imaginary part of the SPAC coefficients calculated from the 'reliable', 'unreliable' and all datasets. In the case of insufficient azimuthal distribution of the stations (linear array) the imaginary part shows some instability and can be regarded as an indicator of insufficient spatial averaging, but when perturbations are associated with insufficient coherency of the wavefield no significant instability is shown. Hence, it is difficult to say definitively that the imaginary part of SPAC coefficients can be regarded as an indicator of data quality, but we need more examples before making a general conclusion.

Acknowledgments

We are grateful to Professor Michael Asten for valuable comments and suggestions. The comments of the Associate Editor, Dr Binzhong Zhou and reviewer Professor Anderson helped us to improve the manuscript. We thank Mr. Chisato Konishi and Mr. Toru Suzuki who helped us for conducting array observation. The authors also express their gratitude to the Japan Society for the Promotion of Science for financial support during the period of this study.

References

Aki, K., 1957, Space and time spectra of stationary stochastic waves, with special reference to microtremors: *Bulletin of the Earthquake Research Institute*, **35**, 415–456.

Asten, M. W., 2006, On bias and noise in passive seismic data from finite circular array data processed using SPAC methods: *Geophysics*, **71**, V153–V162. doi: 10.1190/1.2345054

Asten, M. W., and Henstridge, J. D., 1984, Array estimators and the use of microseisms for reconnaissance of sedimentary basins: *Geophysics*, **49**, 1828–1837. doi: 10.1190/1.1441596

Capon, J., 1969, High-resolution frequency-wavenumber spectrum analysis: *Proceedings of the Institute of Electrical and Electronics Engineers*, **57**, 1408–1418.

Chavez-Garcia, F. J., Rodriguez, M., and Stephenson, W. R., 2006, Subsoil structure using SPAC measurements along a line: *Bulletin of the Seismological Society of America*, **96**, 729–736. doi: 10.1785/0120050141

Horike, M., 1985, Inversion of phase velocity of long-period microtremors to S-wave-velocity structure down to the basement in urbanized area: *Journal of Physics of the Earth*, **33**, 59–96.

Ingber, L., 1989, Very fast simulated reannealing: *Mathematical and Computer Modelling*, **12**, 967–973. doi: 10.1016/0895-7177(89)90202-1

Ling, S., and Okada, H., 1993, An extended use of the spatial autocorrelation method for the estimation of geological structure using microtremors: *Proceedings of the 89th SEGJ Conference,* 44–48 (in Japanese).

Margaryan, S., 2006, Determination of S-wave velocity structure using array microtremor measurements: conventional and two-site spatial autocorrelation method: *Proceedings of the First European Conference on Earthquake Engineering and Seismology*, Paper No. 478.

Morikawa, H., Sawada, S., and Akamatsu, J., 2004, A method to estimate phase velocities of Rayleigh waves using microseisms simultaneously observed at two sites: *Bulletin of the Seismological Society of America*, **94**, 961–976. doi: 10.1785/0120030020

Ohori, M., Nobata, A., and Wakamatsu, K., 2002, A comparison of ESAC and FK methods of estimating phase velocity using arbitrarily shaped microtremor arrays: *Bulletin of the Seismological Society of America*, **92**, 2323–2332. doi: 10.1785/0119980109

Okada, H., 1998, *Microtremors as an exploration method:* Geo-exploration Handbook, vol. 2, Society of Exploration Geophysicists of Japan.

Okada, H., 2003, *The microtremor survey method* (translated by Koya Sato): Geophysical monograph series, No. 12, Society of Exploration Geophysicists.

Okada, H., 2006, Theory of efficient array observations of microtremors with special reference to the SPAC method: *Exploration Geophysics*, **37**, 73–85. doi: 10.1071/EG06073

Okada, H., Matsuhima, T., Moriya, T., and Sasatani, T., 1990, An exploration technique using long-period microtremors for determination of deep geological structures under urbanized areas: *Butsuri Tansa*, **43**, 402–417.

Suzuki, H., and Takahashi, T., 1999, S-wave Velocity Survey in Tsukuba City by Array Microtremor Measurements – Comparison with deep borehole data: *Proceedings of the 101st SEGJ Conference*, 50–53.

Tsuno, S., and Kudo, K., 2004, On the efficiency and precision of array analysis of microtremors by the SPAC method in practical engineering use: *The 13th World Conference on Earthquake Engineering*, Vancouver, B.C., Canada, Paper No. 345.

Yamanaka, H., 2004, Application of heuristic search methods to phase velocity inversion in microtremor array exploration: *Conference Proceedings of the 13th World Conference of Earthquake Engineering*, Paper No. 1161.

Yamanaka, H., and Ishida, H., 1996, Application of genetic algorithms to an inversion of surface-wave dispersion data: *Bulletin of the Seismological Society of America*, **86**, 436–444.

Yokoi, T., 2005, Combination of Down Hill Simplex Algorithm with Very Fast Simulated Annealing Method – An effective cooling schedule for inversion of surface wave's dispersion curve: *Proceedings of the Fall Meeting of Seismological Society of Japan.* B049.

Manuscript received 2 November 2007; revised manuscript received 24 September 2008.

SPAC 法と直線アレイ法の安定性、及び微動記録の質の指標としての SPAC 係数の虚部に関する野外実験

ソス マルガリャン[1,3]・横井俊明[1]・林　宏一[2]

1 建築研究所国際地震工学センター
2 応用地質（株）
3 現在、アルメニア共和国イェレバン国立大学地質学部

要　旨： 近年Ｓ波速度構造の推定に使われている微動のアレイ観測の内、従来の空間自己相関法（ＳＰＡＣ）では、最低３ないし４個の地震計による同時観測が必要である。その変形である 2sSPAC や直線アレイ法では 2 個のみの地震計により S 波速度構造の推定が可能であるが、1.0Hz 以上の周波数帯では空間自己相関係数の不安定さの悪影響を受ける。この研究では、四つの異なるサイズの正三角形アレイと四つの同一サイズの正三角形アレイ及び直線アレイによる微動観測に基づき、2Hz から 4 ないし 5Hz までの周波数帯でのＳＰＡＣ係数の安定性を示す。これらのアレイ観測は PS-logging 記録のある地点の近傍で連続した互いに異なる時間窓で実施され、直線アレイの場合を除き、全ての記録はＳＰＡＣ法で解析された。ＳＰＡＣ係数をベッセル関数にフィッティングすることで得られる位相速度は、これらのアレイ間では 5Hz まで調和的であった。加えて、ＳＰＡＣ係数の虚部が微動記録の質の指標となり得るか、を調べた。自己相関スペクトルの擾乱の具合（また微動波形記録の視認により）、微動記録を、「信頼可」、「信頼不可」の二分類に分け、これらと「完全」（前二者を合わせたもの）に対してＳＰＡＣ係数の虚部を計算し結果を比較した。観測点の方位分布が不十分な場合（直線アレイ）、ＳＰＡＣ係数の虚部はいくらかの不安定を示し、それゆえ方位平均の不十分さの指標になり得る。しかし、低コヒーレンスの波動場においても、ＳＰＡＣ係数の虚部は意味のある不安定さは示さなかった。

キーワード：微動，空間自己相関法，直線アレイ，安定性，SPAC 係数の虚部

공간자기상관법 (SPAC)의 안정성과 선형 배열법과 자료 품질 지시자로 활용되는 SPAC 계수의 허수 성분에 대한 실험

Sos Margaryan[1], Toshiaki Yokoi[1], Koichi Hayashi[2]

1 건축 연구소 국제 지진 공학 연구소
2 응용 지질 (주)

요 약： 최근 상시 진동 탐사법은 횡파 속도 구조의 규명을 위하여 이용되고 있다. 상시 진동 탐사법 중 공간자기상관(SPAC)법은 적어도 3 혹은 4개의 수신기에서 동시에 기록된 자료를 이용한다. 2sSPAC과 선형 배열 상시 진동법과 같은 수정된 SPAC법은 2개의 수신기 자료만 이용하여 횡파 속도를 추정할 수 있지만, 1.0 Hz 이상의 주파수 대역에 대한 공간 자기상관 계수가 불안정해지는 문제점을 가지고 있다.

4개의 서로 다른 크기의 삼각형 배열과 4개의 같은 크기의 삼각형 및 선형 배열을 이용한 상시 진동 측정치에 근거하여, 2 Hz 에서 4 Hz 혹은 5 Hz 주파수 대역에 대한 SPAC 계수의 안정성을 증명하였다. SPAC 계수를 Bessel 함수로 회귀하는 방식으로 획득되는 위상속도는 5 Hz까지 일관성을 보여주었다. 공간평균법을 이용한 선형배열의 경우를 제외하고, 모든 자료는 SPAC법으로 처리되었다. 평행탄성파법 자료가 있는 시추공 주변에서 상시 진동 배열을 순차적으로 다른 시간에 적용하였다.

자료의 품질을 나타내는 지시자로 SPAC 계수의 허수 성분을 이용하였다. 자기상관 스펙트럼의 변화량 (어떠한 경우에는 기록된 파동장에 대한 육안 검사) 에 근거하여, 측정된 자료를 ‘신뢰성있는(reliable)’과 ‘신뢰성이 없는(unreliable)’로 구분하였다. 그 후, ‘reliable’과 ‘unreliable’로 구분된 자료와 모든 자료에 대하여 SPAC 스펙트럼의 허수 성분을 계산하고 비교하였다. 측점의 방위각 분포가 불충분한 경우 (선형 배열), 허수 성분 곡선은 불안정한 형태를 나타내었고, 이러한 결과는 불충분한 공간평균의 지시자로 간주할 수 있음을 의미한다. 하지만, 측정된 파동장이 낮은 일관성을 나타낼 경우에도 허수성분 곡선은 주목할 만한 불안정성을 나타내지 않았다.

주요어：공간 자기상관 계수의 허수 성분, 선형 배열, 상시 진동, 공간 자기상관, 안정성